

THE ELECTRON-CLOUD INSTABILITY IN PEP-II[†]

M. A. Furman and G. R. Lambertson, LBNL mail stop 71–259, Berkeley, CA 94720, USA

Abstract

Any intense positively-charged beam creates a cloud of electrons in the vacuum chamber. This cloud couples the transverse motions of the bunches, potentially leading to an instability. In this paper we report on estimates for such an effect for the positron beam in the PEP-II collider, obtained by means of simulations. We specify quantities upon which the magnitude and shape of the electron cloud density distribution depend sensitively. We pay particular attention to the secondary electron emission process, which plays an important role in this case. A low-emission coating alleviates the problem considerably. Although our calculation is still in progress, we conclude that the instability rise time is > 0.4 ms, which is within the range controllable by the feedback system.

1 INTRODUCTION

Accumulation of electrons was observed to produce a beam-induced multipactoring in the ISR [1]. A new effect attributed to electrons has been seen at the Photon Factory (PF) at KEK when operating with a multibunch positron beam [2]. This is a fast coupled-bunch instability that disappears only when the bunch spacing becomes sufficiently large. Experimental analyses [2] and simulations [3] strongly suggest that the origin of this instability is the electron cloud, which couples the transverse motion of successive bunches.

It has been conjectured that the electron cloud might also have been responsible for the “multi-mode instability” seen at DORIS [4] in the past. Another instance in which electrons are implicated in a multi-bunch instability is in the CESR collider [5], in which it is known that electrons trapped in the chamber by the combined magnetic field of the bending dipoles and the electric leak fields from the distributed ion pumps couple the motion of successive bunches. In this case, however, the electron cloud is localized to the regions near the pumps and thus occupies a small fraction of the ring circumference. In the case of the ISR and the PF (and, presumably, DORIS), the electron cloud occupies essentially the entire ring circumference.

In this article we report on the results from the simulation code “POSINST” that is being developed to study the electron-cloud effect that is expected in the positron beam of the PEP-II B factory [6], now under construction at SLAC. A full report will be available in the future [7]. An analytic approach has also been carried out under simplifying assumptions [8] whose results are in qualitative agreement with those from POSINST if restricted by the same assumptions.

We have developed the simulation in the same spirit as

reported in Ref. 3, except that we have included the secondary electron emission effect in a fair amount of detail, because it is important in the PEP-II parameter regime. So far the code POSINST has been optimized to produce a reasonably accurate determination of the electron cloud density distribution. Once we have the equilibrium distribution, we perturb it by vertically displacing one bunch by a fixed amount and observing the effect on successive bunches. From this we estimate the dipole wake function, and from it we obtain the instability risetime from standard formulas [9].

We have studied separately the electron cloud in the pumping straight sections and in the dipole bending magnets; these two elements comprise most of the ring structure. On average, the electron density in the magnets is higher than in the pumping straight sections. The combined weighted average for the growth rate gives an estimate $\tau > 0.4$ ms. We have not yet incorporated the space-charge effects from the electron cloud on the dynamics of the instability; however, these effects are beneficial, in the sense that they tend to make the growth rate lower. For this reason (and others to be discussed below) the above-mentioned estimate of 0.4 ms is a lower bound. Nevertheless, the calculation is far from complete, and much work remains to be done to arrive at a more reliable calculation of the growth time.

2 SIMULATION CODE

In the simulation we assume that there is a periodic source of photoelectrons produced by the photons from the synchrotron radiation generated as each positron bunch goes through every bending magnet. The PEP-II vacuum chamber has an antechamber on the outer-radius side through which most of the synchrotron radiation escapes and has no effect for our purposes. Nevertheless, a few soft photons strike the vacuum chamber wall just above and just below the antechamber slot with an average energy of ~ 5 eV and a grazing angle of ~ 1 mrad. On average, each positron in any given bunch generates ~ 0.05 such photons per dipole bending magnet. At these angles and energies the photons do not create photoelectrons when they first hit the chamber because the specular reflectivity is $> 90\%$ [10]. This means that the photons will bounce many times before generating photoelectrons. In the process, they get distributed fairly uniformly around the chamber, and so the photoelectrons are also distributed uniformly. Each bunch yields photons that are generated gaussianly in time with an rms width of 33 ps, reflecting the gaussian shape of the positron bunch, whose rms length is 1 cm. Since the positron bunch spacing is 1.26 m, the photoelectrons are produced periodically with a frequency of 238 MHz.

On average, we assume that each photon yields 0.1 photoelectrons. Thus, for the nominal charge of 5.6×10^{11} positrons per bunch, an average of $\sim 0.1 \times 0.05 \times 5.6 \times 10^{11} = 2.8 \times 10^9$ photoelectrons are generated per positron bunch passage in the region downstream from a dipole magnet. It

[†]Work supported by the Director, Office of Energy Research, Office of High Energy and Nuclear Physics, High Energy Division, of the U.S. Department of Energy under Contract no. DE-AC03-76SF00098.

is unrealistic to simulate such a large number of photoelectrons; thus, in practice, the simulation starts with a fixed number of photoelectrons per bunch passage, typically 1000, and follows these in time for up to 1000 bunch passages.

The photoelectrons are generated gaussianly in time with an rms width of 33 ps, reflecting the photon time distribution. Their typical energy is comparable to that of the photons, namely ~ 5 eV. They are then kicked transversely by the successive bunches that go by. As they hit the opposite side of the chamber, they can get absorbed or generate secondary electrons that are, in turn, kicked by the bunch train. If the secondary emission were high enough, the positron ring would function like a gigantic photoamplifier. In the following section we discuss more details of the secondary emission process.

The PEP-II vacuum chamber has an elliptical cross-section of semi-axes $(a,b)=(4.5,2.5)$ cm. As mentioned above, there is an antechamber slot of full height 1.5 cm on the outer-radius side. This geometry is incorporated in our simulation. The electron cloud kinematics is fully three-dimensional. As mentioned above, we have not yet included the effects from the space-charge forces from the electron cloud. Thus the electrons are assumed to move independently of each other. The space-charge forces can only be beneficial because they reduce the energies of the electrons incident on the wall and thus suppress secondary emission.

3 SECONDARY EMISSION

When an electron strikes a metallic surface it can be either absorbed, or backscattered elastically, or rediffused and then ejected back, or interact in a more complicated way with the metal and generate “true secondary” electrons. The basic quantity that describes the process is the secondary emission yield (SEY) δ , which is, by definition, the average number of ejected electrons per incident electron (δ contains the contributions of the elastically backscattered, rediffused, and true secondaries). Because this yield is critical in determining the equilibrium state of the electron cloud, the quantity that is needed for the simulation is not δ itself but rather the probability

$$\frac{dP_n}{d^3 p_1 d^3 p_2 \cdots d^3 p_n} \quad (1)$$

that an incident electron with energy and angle (E_0, θ_0) will generate n secondaries with momenta $\mathbf{p}_1, \mathbf{p}_2, \dots, \mathbf{p}_n$. As far as we know, such details are not known experimentally or theoretically. However, based on a large body of phenomenology [11] and theory [12], we have developed a model [7] for the differential probability, Eq. (1), that is consistent with the experimental data. This model is obviously far from unique, but we have tested the dependence on unknown model parameters and concluded that the results of our simulations do not change qualitatively in the regime of interest for the PEP-II positron ring provided the basic parameters of the SEY are kept fixed.

Most pure metals have a maximum value of the SEY, δ_{\max} , in the range 0.9–1.3. The PEP-II vacuum chamber is made of aluminum, which has $\delta_{\max} \approx 0.9$ in pure form,

one of the lowest values of all (amorphous) metals. Unfortunately, aluminum is normally covered with a crust of Al_2O_3 , which has $\delta_{\max} \approx 2.5$, which is among the highest of all metals. Our simulation results have shown that such a value of δ_{\max} would probably lead to a very unfavorable situation vis-a-vis the electron cloud instability. As a result, we have decided to coat the chamber with a substance such as TiN, which has a more typical value $\delta_{\max} \approx 1.14$. In all results presented here, we shall assume, unless otherwise noted, that the chamber is coated with a TiN layer a few hundred Å thick (many other kinds of coating would work just as well).

4 RESULTS

For the present purposes, we assume a very simplified model for the ring, composed of nothing but 192 dipole bending magnets and 192 pumping straight sections. The magnets have a length of 45 cm, a field of 0.752 T, and an orbit curvature radius of 13.75 m, corresponding to the beam energy of 3.1 GeV. The pumping straight sections are 5 m long, and have no strong magnetic field.

The simulation shows that the electron cloud is fully established within ~ 20 bunch passages after the first bunch in the train goes by. By the same token the cloud disappears after ~ 20 empty buckets go by. Since the PEP-II beam will operate with a gap equivalent to 88 bunches, we conclude that the cloud effectively disappears at any point in the ring during the passage of the gap. As a consequence, there is no turn-to-turn coupling, and the electron cloud multibunch instability resembles more the beam breakup instability in linacs than a typical multibunch instability in circular machines. A leading bunch drives a trailing bunch whose amplitude then grows algebraically in time rather than exponentially [9].

4.1 Pumping straight sections

In this case the electrons hit the wall with an average energy ~ 1 keV. In spite of this large value, it turns out that the otherwise broad collision energy spectrum has a sharp, tall peak at ~ 50 eV, where δ is well below unity. Also, the spectrum of the collision angles is sharply peaked about normal incidence. These numbers combine into an effective SEY $\delta_{\text{eff}} \approx 0.6$. Since this is < 1 , it means that there is preferential absorption in the walls, and the number of electrons in the cloud reaches a stable equilibrium when the average number of absorbed electrons per bunch passage equals the number of photoelectrons generated per bunch passage. The resultant average density is $\sim 5 \times 10^5$ e/cc. This low value justifies ignoring the space-charge effects in this case. The shape of the density is quite uniform, and its contour level plot is shown in Fig. 1.

By perturbing the trajectory of a specific bunch we obtain the dipole wake function at the location of the next bunch. The result is $W_1 < 30 \text{ m}^{-2}$, which yields a growth rate $\tau^{-1} < 0.5 \text{ ms}^{-1}$. Mathematically, this value corresponds to a “ring” wholly composed of pumping straights. The reason for the inequality in the numbers above is that we were not able to distinguish the perturbation on the trailing bunch from the statistical noise in the simulation (the code does show a clear signal when certain parameters are pushed beyond the nominal values for PEP-II). In addition, as mentioned earlier, the

space-charge forces are expected to have a further effect of decreasing τ^{-1} , although this will not be significant for the pumping straights.

4.2 Dipole bending magnets

In this case the magnetic field confines the electrons in the cloud to move in tight vertical helices whose radius is typically a fraction of a mm. The electron density has high peaks along vertical sheets on either side of the beam, as shown in Fig. 1. It turns out that, in this case, δ_{eff} is slightly larger than 1, and so, in our present simulation, the number of electrons trapped in the dipoles grows exponentially without bound. Thus the cloud density will reach an equilibrium state only thanks to the space-charge force which, as we said earlier, is not yet included in the present simulation. The key difference with the situation in the pumping straights is that the collision angle is widely distributed over all angles, and this causes δ_{eff} to be higher than in the pumping straights (the spectrum of the collision energies is similar in the two cases).

To allow the estimation of a growth rate, we assume that the number of electrons in the cloud will reach a maximum that corresponds to a fully neutralized beam (an average of 1.3×10^7 e/cc). Scaling our results to this limit, the resultant wake function at a distance of one bunch spacing is $W_1 < 1300 \text{ m}^{-2}$, and the corresponding growth rate is $\tau^{-1} < 25 \text{ ms}^{-1}$. This is the growth rate that would obtain if the ring were composed only of such dipoles. Again, this is an upper bound on the rate because of the same reasons mentioned above. It is clear that the space charge force plays an important role in this case.

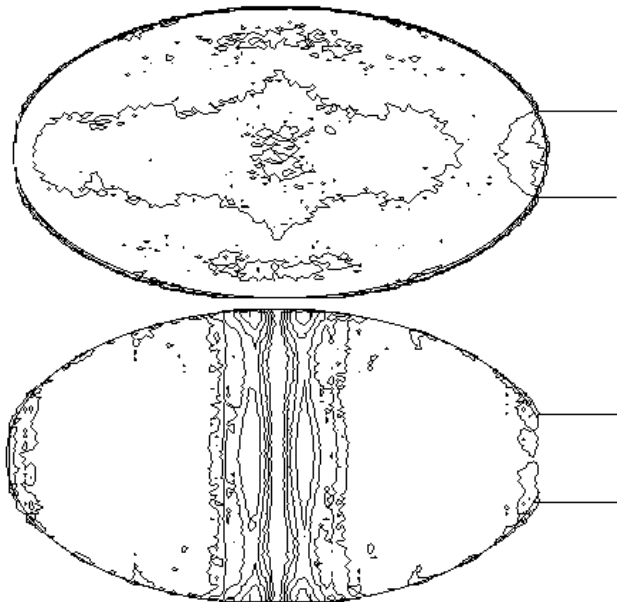


Fig. 1. Contour level plots of the electron cloud. Top: pumping straight section. Bottom: dipole bending magnet. The beam orbit is at the center of the ellipse. The antechamber slot is shown at the right-side of the chamber. The ratio between successive levels is 2, and the top level is at 99% of the peak.

5 CONCLUSIONS

We estimate the overall instability growth rate for our

model ring from the weighted average from the pumping straights and the bending dipoles, obtaining

$$\tau^{-1} < 0.5 + 2.1 = 2.6 \text{ ms}^{-1} \quad (2)$$

where the first number (0.5) is the weighted contribution from the pumping straights, and the second (2.1) from the dipoles. This implies $\tau > 0.4 \text{ ms}$, which is within the range controllable by the PEP-II feedback system.

We have learned from the simulation that it is important to use the proper formula for the electromagnetic field produced by the positron bunch that fulfills the elliptic-chamber boundary conditions. The usual Bassetti-Erskine [13] formula for the field, corresponding to free space, gives significantly different results. We have also learned that, in computing the dipole wake function, it is important to take into account the image charges of the electrons in the cloud.

The electron cloud average density and shape of the distribution is sensitive to the chamber geometry, bunch current and spacing, dipole field, and chamber surface material. In addition, since the electron cloud dynamics is quite fast, it seems unlikely, at least for now, that one can find simple scaling rules from which one might extrapolate results from one machine to another.

6 ACKNOWLEDGEMENTS

We are grateful to the LBNL PEP-II group for many discussions.

7 REFERENCES

- [1] O. Gröbner, Proc. 10th Intl. Accel. Conf., Serpukhov, 1977, p. 277; R. S. Calder, Vacuum **24** (10), 437.
- [2] M. Izawa, Y. Sato and T. Toyomasu, Phys. Rev. Lett. **74**, 5044 (1995).
- [3] K. Ohmi, Phys. Rev. Lett. **75**, 1526 (1995).
- [4] G. A. Voss, Proc. 1975 PAC, Washington, DC, p. 1363.
- [5] J. Rogers, Proc. 1995 PAC and ICHEA, Dallas, TX, p. 3052.
- [6] *PEP-II: An Asymmetric B Factory—Conceptual Design Report*, June 1993, LBL-PUB-5379/SLAC-418/CALT-68-1869/UCRL-ID-114055/UC-IIRPA-93-01.
- [7] M. A. Furman and G. R. Lambertson, to be published.
- [8] S. Heifets, PEP-II AP Note 95.21, June 7, 1995; SLAC/AP-95-101, October 1995.
- [9] A. W. Chao, Physics of Collective Beam Instabilities in High Energy Accelerators, J. Wiley, 1993.
- [10] J. Kirz et al, eds., *X-ray data booklet*, LBL-PUB-490, April 1986.
- [11] See, e.g., P. A. Redhead, J. P. Hobson and E. V. Kornelsen, *The Physical Basis of Ultrahigh Vacuum*, Chapman and Hall, Ltd., 1968, ch. 4. H. Bruining, *Physics and Applications of Secondary Electron Emission*, Pergamon Press, 1954.
- [12] See, e.g., H. Seiler, J. Appl. Phys. **54**, R1 (Nov. 1983).
- [13] M. Bassetti and G. A. Erskine, CERN-ISR-TH/80-06.